

## COMMUNICATIONS

Calibration of the Stray Field Gradient by a Heteronuclear Method and by Field Profiling<sup>1</sup>

Alasdair R. Preston, Paul Kinchesh, and Edward W. Randall

*Department of Chemistry, Queen Mary & Westfield College, University of London, London E1 4NS, United Kingdom*

Received March 20, 2000; revised July 18, 2000

**Heteronuclear and field-profiling stray field (STRAFI) techniques are used to calibrate the STRAFI gradient. Both methods compare very favorably indeed with the conventional method of calibration which uses a standard with a known self-diffusion constant. The distinct advantages of the techniques presented here are that the constraints on both sample purity and sample temperature that are inherent to the conventional method are completely eliminated. The accuracy of the heteronuclear method typically matches that of the conventional method with a pure sample and temperature stability to within 0.4°C. The field-profiling method is more accurate than the heteronuclear method in the form that it is presented here.** © 2000 Academic Press

**Key Words:** stray field; STRAFI; fringe field; gradient calibration.

The strong field-gradients in the stray field (STRAFI) or fringe-field of super-conducting solenoids, which are on the order of 10–100 T/m, are useful for studies of very slow self-diffusion and for the imaging of substances with very broad line shapes, such as polycrystalline solids. Each of these uses of the STRAFI technique has been reviewed recently (1–4). The excited part of the sample is a narrow slice, with a thickness on the order of 10–100 μm for protons, about Samoilenko's "sensitive plane" (5).

The self-diffusion application requires accurate knowledge of the field gradient at the position of the measurement. Normally the gradient for self-diffusion experiments is calibrated by a measurement on a substance of known self-diffusion constant, or reliance is placed on the calculated gradient for the field distribution of the magnet. Surprisingly, no attention is given to this facet of the experiment in the otherwise excellent article by Geil (1). The self-diffusion method requires a standard substance which ideally can be easily purified, and which has a known self-diffusion constant with a small temperature coefficient.

An accurate knowledge of the value of the gradient is not normally required for imaging purposes. The function of the gradient here is simply to dominate the spin Hamiltonian in the so-called high field-gradient approximation (5). Generally one can neglect the chemical screening and the nuclear couplings both direct and indirect and even modest quadrupolar interactions.

We propose here two methods for gradient calibration, both of which make use of STRAFI imaging techniques: a STRAFI heteronuclear method and a STRAFI field-profiling method.

For two heteronuclei at a fixed frequency, there are two "sensitive planes," which are displaced in space because of the difference in the gyromagnetic ratios,  $\gamma_n$ . The separation ( $d$ ) depends upon the field-profile: larger magnetic fields ( $B_0$ ) increase  $d$ , whereas larger gradients ( $G$ ) decrease it.

At a fixed frequency,  $\omega$ , for the fluorine and proton nuclei in a linear gradient,  $d$  is given by

$$d = \frac{\omega}{G} \left( \frac{1}{\gamma_F} - \frac{1}{\gamma_H} \right) \quad [1]^2$$

Consequently, a phantom containing both these nuclei in a single substance gives a STRAFI 1D projection consisting of two images that are displaced by  $d$  (6). These images will not overlap provided that the projection of the phantom on the  $z$ -axis of  $B_0$  is less than  $d$ . All that is required for the calibration of the gradient is an accurate measurement of the displacement of the images.

The two images can be obtained in one pass of the translational motion which scans the phantom through the "sensitive planes" in the same fashion as for conventional STRAFI imaging techniques, as shown in Fig. 1: the 1D image is a record of the signal detected as a function of time as the sample is moved stepwise along the  $z$ -axis of  $B_0$  (6).

For calibration purposes the most convenient pair of nuclides is <sup>1</sup>H and <sup>19</sup>F which have gyromagnetic ratios which differ by about 6%. For some other pairs of nuclides, such as

<sup>1</sup> A preliminary account of this work was presented at the 5th International Conference on Magnetic Resonance Microscopy and Macroscopy, Heidelberg, 1999.

<sup>2</sup> The equation in Ref. (6) is incorrect due to a typing error.

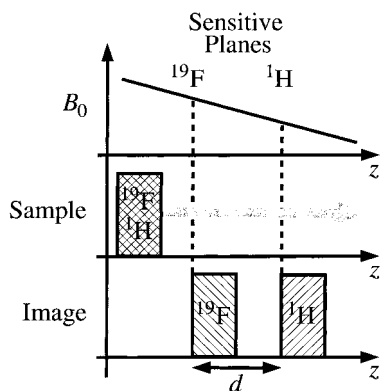


**FIG. 1.** Diagrammatic representation of the 1D STRAFI image generated by stepwise movement of a phantom containing  $^1\text{H}$  and  $^{19}\text{F}$  nuclei through the two “sensitive planes” that are excited by the application of RF pulses at a fixed frequency. The displacement  $d$  between the  $^1\text{H}$  and  $^{19}\text{F}$  images allows the magnitude of the STRAFI gradient  $G$  to be calculated from Eq. [1].

$^{23}\text{Na}$  and  $^{27}\text{Al}$ ,  $d$  can be very small because the  $\gamma$  values are very close, and other methods need to be employed to distinguish the overlapping images, such as relaxation time weighting. The absence of a sufficient  $\gamma$ -displacement to enable different nuclides to be distinguished is exacerbated at high values of  $G$ .

We also calibrated the gradient by a STRAFI adaptation of the usual homonuclear field-profiling method. In this method the frequency is changed stepwise to bring a single signal, commonly the proton signal of water, into resonance at different positions in the field. STRAFI imaging techniques were used to produce 1D profiles at each of the frequencies.

For heteronuclear gradient calibration we used a more complex phantom than the one shown in Fig. 1 that contained mainly PMMA and PTFE (i.e., materials which contained either protons or fluorine, but not both). For the field-profiling experiments a proton phantom consisting of four silicone rubber disks separated by three glass-spacers was used and the 1D STRAFI projections were recorded at seven different frequencies over a 11 MHz range about the theoretical optimum frequency of 111.5 MHz. This frequency corresponds to the theoretical optimum position in the stray field along the  $z$ -axis at which the “sensitive plane” shows minimum curvature, rather than the position of maximum gradient along the  $z$ -axis. This position was determined using theoretical field-plots supplied by the manufacturer of the magnet, Oxford Instruments. The phantoms used for the two different methods are shown in Fig. 2 and Fig. 3, respectively, along with the experimentally determined 1D projections.

In the heteronuclear experiment at 111.5 MHz the  $^1\text{H}$ – $^{19}\text{F}$  image displacement  $d$  was determined to be  $13.563 \pm 0.063$  mm, and  $G$  was calculated to be  $12.16 \pm 0.06$  T/m from Eq. [1]. For the field-profiling experiment the displacements of the eight distinguishing features of each 1D projection are plotted as a function of  $B_0$  for each of the seven different frequencies in Fig. 4.  $G$  was calculated to be  $12.091 \pm 0.016$  T/m by

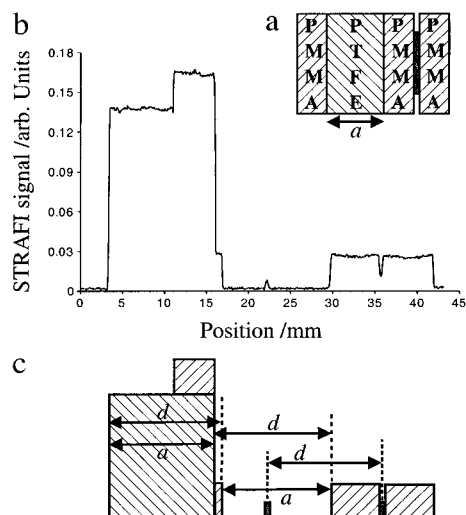


**FIG. 2.** Heteronuclear gradient calibration: (a) Composition of phantom. The unlabelled shaded slice represents a [PTFE film–overhead projector foil–PTFE film] sandwich about  $400 \mu\text{m}$  thick. (b) 1D STRAFI projection of the phantom generated by summing data from  $90_x-t-[90_y-t-\text{echo}-t]_n$  echo trains for each slice. Pulse duration,  $42 \mu\text{s}$ . Echo time,  $120 \mu\text{s}$ . Slice separation,  $90 \mu\text{m}$ . Number of points acquired for each echo, 1 complex pair. Number of echoes in each echo train, 6. Number of slices in projection, 480. Number of averages, 1024. Total imaging time, 11.8 h. The projection presented here was acquired overnight. We expect that a few hours of accumulation would give adequate signal-to-noise. The [PTFE film–overhead projector foil–PTFE film] sandwich could not be resolved. (c) Theoretical 1D STRAFI projection of the phantom.

performing a linear least squares fitting of the data. The errors quoted all correspond to  $\pm 2\sigma$ . Both experimental STRAFI results are in close agreement with the theoretical value of 12.048 T/m determined from the theoretical field-plots.

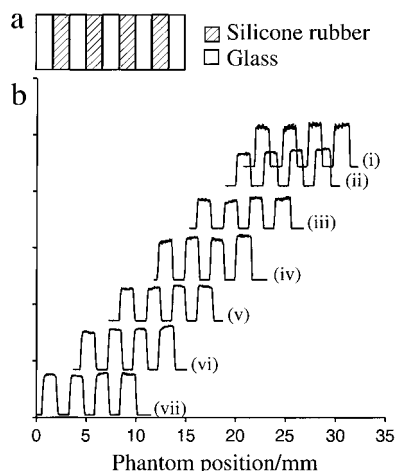


**FIG. 3.** Field-profiling gradient calibration: (a) Composition of phantom. (b) 1D STRAFI projections of the phantom generated by summing data from  $90_x-t-[90_y-t-\text{echo}-t]_n$  echo trains at (i) 106.5 MHz, (ii) 107.5 MHz, (iii) 109.5 MHz, (iv) 111.5 MHz, (v) 113.5 MHz, (vi) 115.5 MHz, and (vii) 117.5 MHz. Pulse duration,  $100 \mu\text{s}$ . Echo time,  $240 \mu\text{s}$ . Slice separation,  $45 \mu\text{m}$ . Number of points acquired for each echo, 16 complex pairs. Number of echoes in each echo train, 64. Number of slices in each projection, 256. Number of averages, 32. Total imaging time, 12 min per profile.

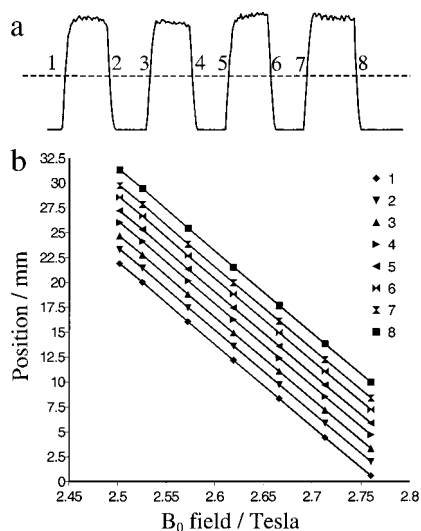


**FIG. 4.** Field-profiling gradient calibration: (a) 1D projection showing the eight distinguishing features given by the half height of the silicone rubber signal (represented here by the intersection with the dashed line). (b) Plot of the displacements of the eight distinguishing features as a function of  $B_0$  for each of the seven different frequencies.

In both methods we used a computerized motor driven STRAFI probe to obtain 1D projections of multiple component phantoms to increase the experimental database and improve the accuracy of the statistical analysis. The version of the heteronuclear (HetN) method we present here uses a single frequency difference produced by the employment of two different nuclides, whereas our modification of the homonuclear field-profiling (HomoNFP) method uses seven different frequencies. The HetN method gives a gradient which is essentially not a tangent to the field profile at the theoretically optimum frequency of 111.5 MHz, but rather is a chord across the field profile between the two sensitive planes. The HomoNFP method uses data acquired over a 11 MHz range about the theoretically optimum frequency of 111.5 MHz and data were fitted by a linear least squares fit over the whole range to give the tangent to the field profile at 111.5 MHz. This analysis assumes that the gradient is constant over the 11 MHz range but the errors generated by this assumption are propagated to give the error with which the value of the gradient has been calculated. Mere inspection of the results presented in Fig. 4 shows the assumption to be very reasonable indeed.

The accuracy with which the gradient can be calculated for both methods depends on the spatial resolution with which the 1D projections are recorded. The spatial resolution is a function of the linewidth, the projection of the excited slice onto the  $z$ -axis, and the resolution of the stepping device. In particular, the linewidths of the observed samples should be as small as possible (7, 8). In terms of spatial resolution this not only makes the linewidth contribution negligible, but also permits the use of longer pulse durations which reduce the size of the projection of the excited slice onto the  $z$ -axis. The projection of

the excited slice onto the  $z$ -axis is also less for nuclides of high  $\gamma$  values, such as  $^1\text{H}$  and  $^{19}\text{F}$ . The edges in the phantom should be parallel to each other and be as normal as possible to the  $z$ -axis of the magnetic field. This is relatively easy to achieve on phantoms of small diameter but we had no troubles with the large, 5 cm, diameter of our phantoms.

Both methods presented here compare very favorably with the more traditional method of using a liquid with known self-diffusion coefficient  $D$ . Suitable liquids are described by Holz and Weingartner (9) who claim an accuracy of 0.3% in the value of  $D$  measured for  $\text{H}_2\text{O}$  at  $25^\circ\text{C}$ . Gradient calibration with this standard would contribute an uncertainty of 0.15% into any calculated gradient value. Moreover,  $D$  is temperature dependent such that to match even the precision of the heteronuclear gradient calibration would require stability at a specific temperature to within  $0.4^\circ\text{C}$ .

The accurate measurement of the gradient in our STRAFI experiments enables calculation of the thickness of the excited slice about the sensitive plane on our STRAFI system in the narrow line limit. For the HetN and HomoNFP experiments presented here the slice thickness is calculated to be 40.0 and  $16.8\ \mu\text{m}$ , respectively, using the equation derived in the theoretical analysis given by Benson and McDonald (10).

It is interesting to note that Eq. [1] is quite general for any spatial distribution of spins. It applies both to the case where the proton and fluorine are in the same molecule and cases where the proton and fluorine are in different separated solids (6). Since  $d$  is frequency dependent it should be possible to separate proton and fluorine contributions by performing experiments over a range of frequencies for any spatial distribution of spins.

The HomoNFP method is inherently more accurate than the HetN, but is more time consuming since it requires repetitive measurements after retuning of the RF coil.

In principle, either technique is preferable to the self-diffusion method since no standard sample is required and there are no constraints on sample purity and temperature stability.

The field-profiles supplied by the manufacturer are probably accurate enough for most purposes.

Experiments were performed on a Varian UNITY Inova high-resolution imaging spectrometer equipped with a 4.7 T, 33 cm horizontal bore Oxford Instruments superconducting magnet. The new STRAFI probe has a double-turn RF saddle-coil on a glass-former which fits inside an RF shielding box. The probe can take samples up to 5 cm in diameter and 8 cm long. The probe assembly is mounted on a platform which can be moved backward and forward in the horizontal plane by a screw driven by a stepper motor. A position encoder is fitted to ensure repeatability of the slice location in the stray field during multiple scans. Sample movement, RF pulsing, and image acquisition are all computer controlled from the spectrometer console. Profiles are obtained by a simple "step and pulse" method rather than continuously during the motion "on the fly" and, currently, adjacent slices are sampled consecu-

tively rather than interleaved as in conventional imaging. Preliminary results show that with the relatively narrow proton lines of PMMA we have achieved a spatial resolution of 100  $\mu\text{m}$  or better for samples that are 5 cm in diameter (11).

### ACKNOWLEDGMENTS

This work was supported by the Bio-technical and Biological Science Research Council through Grant 68/EO8576. The Varian UNITY *Inova* imaging spectrometer was provided by the ULIRS (University of London Intercollegiate Research Service) Scheme and is located in Queen Mary and Westfield College.

### REFERENCES

1. B. Geil, Measurement of translational molecular diffusion using ultrahigh magnetic field gradient NMR, *Concepts Magn. Reson.* **10**, 299–321 (1998).
2. P. J. McDonald and B. Newling, Stray field magnetic resonance imaging, *Rep. Prog. Phys.* **61**, 1441–1493 (1999).
3. P. J. McDonald, Stray field magnetic resonance imaging, *Prog. NMR Spectrosc.* **30**, 69–99 (1997).
4. E. W. Randall, MRI using stray fields, in "Encyclopaedia of Spectroscopy and Spectrometry" (J. C. Lindon, Ed.), pp. 1396–1403, Academic Press, San Diego, (1999).
5. A. A. Samoilenko, D. Y. Artemov, and L. A. Sibeldina, Formation of sensitive layer in experiments on NMR subsurface imaging of solids, *JETP Lett.* **47**, 417–419 (1988).
6. E. W. Randall, A. A. Samoilenko, and T. Nunes, Simultaneous H-1 and F-19 stray-field imaging in solids and liquids, *J. Magn. Reson. A* **117**, 317–319 (1995).
7. E. W. Randall, T. G. Nunes, G. G. Guillot, and P. R. Bodart, T-1-weighting of Hahn echo-trains in the stray-field for deuterium, prospects for imaging using long echo-train summation, *Solid State NMR* **14**, 165–172 (1999).
8. E. W. Randall, A. A. Samoilenko, and R. Fu, Hahn-echoes from N-14 in solids by the stray-field method: prospects for imaging using Long Echo-Train Summation, *Solid State NMR* **14**, 173–179 (1999).
9. M. Holz and H. Weingartner, Calibration in accurate spin-echo self-diffusion measurements using  $^1\text{H}$  and less common nuclei, *J. Magn. Reson.* **92**, 115–125 (1991).
10. T. B. Benson and P. J. McDonald, Profile amplitude modulation in stray field magnetic resonance imaging, *J. Magn. Reson. A* **112**, 17–23 (1995).
11. P. Kinchesh, A. A. Samoilenko, A. R. Preston, and E. W. Randall, "Development of a Large (5 cm) Diameter STRAFI Probe," poster presented at the 5th International Conference on Magnetic Resonance Microscopy and Macroscopy, Heidelberg, 1999. [To be published.]